

Exploring Binary-Neutron-Star-Merger Scenario of Short-Gamma-Ray Bursts by Gravitational-Wave Observation

Kenta Kiuchi,¹ Yuichiro Sekiguchi,² Masaru Shibata,³ and Keisuke Taniguchi⁴

¹*Department of Physics, Waseda University, 3-4-1 Okubo, Shinjuku-ku, Tokyo 169-8555, Japan*

²*Division of Theoretical Astronomy/Center for Computational Astrophysics, National Astronomical Observatory of Japan, 2-21-1, Osawa, Mitaka, Tokyo, 181-8588, Japan*

³*Yukawa Institute for Theoretical Physics, Kyoto University, Kyoto, 606-8502, Japan*

⁴*Department of Physics, University of Wisconsin-Milwaukee, P.O. Box 413, Milwaukee, Wisconsin 53201, USA*

(Received 9 December 2009; published 5 April 2010)

We elucidate the feature of gravitational waves (GWs) from a binary-neutron-star merger collapsing to a black hole by general relativistic simulation. We show that GW spectrum imprints the coalescence dynamics, formation process of disk, equation of state for neutron stars, total masses, and mass ratio. A formation mechanism of the central engine of short- γ -ray bursts, which are likely to be composed of a black hole and surrounding disk, therefore could be constrained by GW observation.

DOI: 10.1103/PhysRevLett.104.141101

PACS numbers: 04.25.D-, 04.30.-w, 04.40.Dg

Introduction.—Coalescence of binary neutron stars (BNSs) is one of the most promising sources for kilometer-size laser interferometric gravitational-wave detectors [1]. It is also a candidate for the central engine of short γ -ray bursts (GRBs), which emit huge energy $\geq 10^{48}$ ergs in a short time scale ~ 0.1 – 1 s [2,3]. According to a standard scenario of GRBs based on the so-called merger scenario, a stellar-mass black hole (BH) surrounded by a hot and massive disk (or torus) should be formed after the merger. Possible relevant processes to extract the energy of this BH-accretion disk system for launching a relativistic jet are neutrino-antineutrino ($\nu\bar{\nu}$) annihilation [4] and/or magnetically driven mechanisms, the so-called Blandford-Znajek process [5]. Studies based on the $\nu\bar{\nu}$ annihilation scenario suggest that an accretion rate of $\dot{M} \geq 0.1M_{\odot}/s$ is required to achieve a sufficiently high energy efficiency [6] and that if the disk had a mass $\geq 0.01M_{\odot}$, it could supply the required energy by neutrino radiation for the duration of ≥ 100 ms [7]. General relativistic magnetohydrodynamic simulations also indicate that if a rapidly rotating BH is formed, its rotational energy can be extracted by the Blandford-Znajek process to achieve a high energy efficiency [8]. However, the merger scenario has not been proven yet observationally, because the counterpart for most of the short GRBs has not been identified [9]. Gravitational waves (GWs) are much more transparent than electromagnetic waves with respect to scattering with matter, and hence, they can propagate from an extremely dense region with negligible scattering. Therefore, GWs can be a valuable observable for determining the central engine of GRBs [10] and for exploring its formation process. This fact motivates us to study the coalescence of BNSs and emitted GWs.

For theoretically studying the late inspiral, merger, and ringdown phases of BNSs, numerical relativity is the unique approach. Simulations of a BNS merger [11–13] suggest that (i) if the total mass of the BNS is smaller than a

threshold mass (M_{thr}) a hypermassive neutron star (HMNS) sustained by rapid and differential rotation is formed after the merger and will survive for more than ~ 100 ms [11], and (ii) otherwise, a BH is formed after the merger in a dynamical time scale ~ 1 ms. In the former case, GW emission [11] or magnetic-field effect such as the magnetorotational instability [14] or neutrino radiation [15] will play an essential role in the subsequent evolution of the HMNS, which will eventually collapse to a BH. Because of the complexity, it will not be an easy task to theoretically clarify the formation process of the BH and gravitational waveforms as well as to accurately predict the launching mechanism of short GRBs. By contrast, in the later case, the formation process of a BH and surrounding disk is primarily determined by the general relativistic hydrodynamics, and magnetic field or neutrino radiation will play a minor role. Reliable theoretical prediction of the merger process and gravitational waveforms by numerical relativity is feasible in this case. Motivated by this idea, we systematically performed numerical relativity simulations to clarify the relation between the possible formation process of the GRB's central engine (a system composed of a BH and surrounding disk) and gravitational waveforms, and suggest that GW observation could constrain the formation process for the central engine of short GRBs.

Method and initial models.—Formulation and numerical schemes for solving Einstein's equations, hydrodynamics, and other techniques such as GW extraction are essentially the same as those in Ref. [13], to which the reader may refer for details. For modeling the equation of state (EOS) of neutron stars, we adopt the Akmal-Pandharipande-Ravenhall (APR) [16], Skyrme-Lyon (SLy) [17], and Friedman-Pandharipande-Skyrme (FPS) [18] EOSs for the zero-temperature part. Shock-heating effect, although it gives only minor contribution, is mimicked by Γ -law EOS with $\Gamma = 2$. BNSs of the irrotational velocity field and zero-temperature in quasiequilibrium circular orbits

are prepared as initial conditions, which are computed by the LORENE library codes [19]. For all the models, the initial orbital separation is large enough that the BNSs spend about 4 orbits in the inspiral phase before the merger. Grid structure and resolution are approximately the same as in Ref. [13]; the major diameter of the neutron stars is covered by about 80 uniform grids and outer boundaries of numerical domain are located at about $1.2\lambda_0$ where λ_0 is initial gravitational wavelength. Total mass, m_0 , is chosen to be large enough that a BH is formed in a dynamical time scale (~ 1 ms) after the onset of the merger. This can be achieved for $m_0 > M_{\text{thr}}$, where $M_{\text{thr}} \approx 2.8\text{--}2.9M_\odot$ for the APR, $\approx 2.7\text{--}2.8M_\odot$ for the SLy, and $\approx 2.5\text{--}2.6M_\odot$ for the FPS EOS, respectively [11]. Total mass and mass ratio are chosen in the range of $2.9M_\odot \leq m_0 \leq 3.1M_\odot$, $0.8 \leq \nu \equiv m_1/m_2 \leq 1$ for the APR, $2.8M_\odot \leq m_0 \leq 3.0M_\odot$, $\nu = 1$ for the SLy, and $2.6M_\odot \leq m_0 \leq 2.8M_\odot$, $\nu = 0.8$ and 1 for the FPS EOS. m_1 and m_2 ($m_2 \geq m_1$) denote the gravitational mass of two neutron stars in isolation and $m_0 = m_1 + m_2$. We name the models according to the EOS, m_0 , and ν ; e.g., A2.9-0.9 is modeled by the APR EOS with $m_0 = 2.9M_\odot$ and $\nu = 0.9$.

Results.—We investigate the relation between GWs and the possible formation process of a BH-disk system in a wide range of parameter space. First of all, we briefly review a typical coalescence process of BNSs collapsing dynamically to a BH (see Ref. [13] in details). During the inspiral phase, the BNSs adiabatically evolve gradually decreasing its orbital separation due to the gravitational radiation reaction. GWs in this phase are characterized by a chirp signal (see the waveform for $t_{\text{ret}} - t_{\text{merge}} \lesssim 0$ in Fig. 1). After the binary separation becomes $\lesssim 3$ neutron star radii, the merger sets in. For $\nu \approx 1$, a high-density region with density $> 10^{15}$ g/cm³ is subsequently formed at the center, and then, collapses to a BH within ~ 1 ms. During this merger process, small spiral arms, composed of

two symmetric arms, are formed around the BH but they are eventually swallowed by the BH. The final outcome is a rotating BH nearly in a vacuum state. For $\nu \leq 0.9$, the less massive star is tidally deformed in a close orbit and disrupted just after the onset of the merger. The outer part of the tidally disrupted neutron-star matter forms an asymmetric spiral arm which is more massive and widely spread than that for the equal-mass case. Although the central high-density region, formed at the onset of the merger, collapses to a BH, the large spiral arm subsequently forms an accretion disk around the BH because it has angular momentum large enough to escape from the capture by the BH. GWs in the merger phase are characterized by the short-term burst-type waves ($0 \leq t_{\text{ret}} - t_{\text{merge}} \leq 1$ ms in Fig. 1) and after the BH formation, quasinormal modes (QNMs) are excited ($t_{\text{ret}} - t_{\text{merge}} \geq 1$ ms in Fig. 1). Figure 1, which plots GWs for A2.9-0.8, S2.8-1, and F2.6-0.8 and shows typical waveforms for the BNS merger, illustrates features mentioned above.

The GW spectrum more clearly reflects dynamics of the merger process. Figure 2 plots an effective amplitude of GWs as a function of the frequency, $h_{\text{eff}}(f)$, for models A2.9-0.8, A2.9-1, S2.8-1, F2.6-1, and F2.6-0.8. The effective amplitude is defined by $h_{\text{eff}} \equiv \tilde{h}(f)m_0/D$ with $\tilde{h}(f)$ being the Fourier transform of $h_+ + ih_\times$. We assume that the distance from the observer to the source is $D = 100$ Mpc, because more than one event per year is predicted for such a large distance [20]. Note that GW frequency increases as the orbital separation decreases and as the compactness of the merged object increases: GWs with $f \lesssim 1$ kHz, $1 \lesssim f \lesssim 3$ kHz, and $f \gtrsim 3$ kHz are emitted in the inspiral phase, early merger, and late merger phases, respectively.

The effective amplitude gradually decreases for $f \lesssim 3$ kHz according to $\propto f^{-n}$ with $n \approx 1/6$ which is the typical number for the inspiral phase, and for $f \gtrsim f_{\text{cut}} \approx 2.5\text{--}4$ kHz, its gradient becomes steep (see the small panel

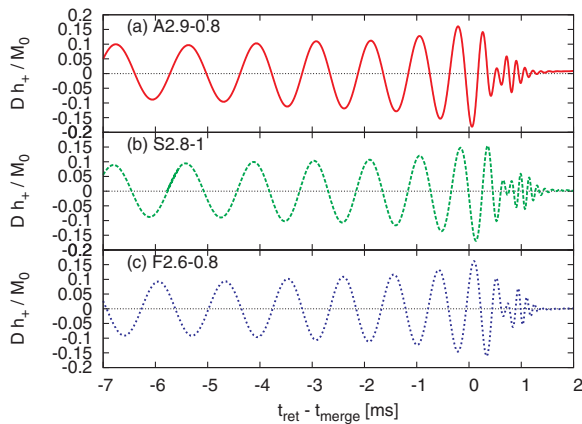


FIG. 1 (color online). + modes of GWs for (a) A2.9-0.8, (b) S2.8-1, and (c) F2.6-0.8. D is the distance from the source to the observer, who is located along the axis perpendicular to the orbital plane. t_{merge} denotes approximate time at the onset of the merger.

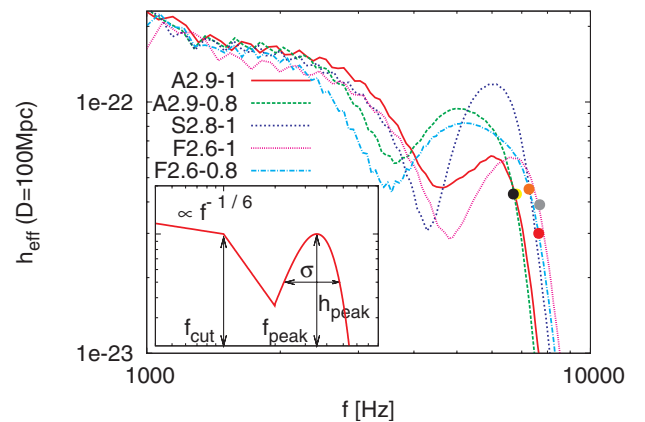


FIG. 2 (color online). Effective amplitude for models A2.9-1, A2.9-0.8, S2.8-1, F2.6-1, and F2.6-0.8. The filled circles denote the QNM frequency of the formed BHs. The small panel shows a schematic figure of the GW spectrum.

in Fig. 2 for $f \gtrsim f_{\text{cut}}$. For $f \lesssim f_{\text{cut}}$, the merged object has a binarylike structure (i.e., there exist two density maxima) which enhances emissivity of GWs, whereas at $f \sim f_{\text{cut}}$, such structure is disrupted, resulting in a quick decrease of the GW amplitude. A hump, which appears for $4 \lesssim f \lesssim 7$ kHz with the peak frequency $f_{\text{peak}} \sim 5\text{--}6$ kHz, reflects the formation and evolution of the spiral arms orbiting the central object. For $f > f_{\text{peak}}$, h_{eff} exponentially decreases; this is the typical feature for the spectrum associated with a QNM ringdown of the formed BH. These spectrum features are qualitatively universal as shown in Fig. 2. However, the spectrum shape depends quantitatively on the EOS, m_0 , and ν .

The spectrum shape for $f \gtrsim f_{\text{cut}}$ is characterized by f_{cut} , f_{peak} , and peak amplitude and width of the hump (h_{peak} and σ), for which a schematic figure is described in the small panel of Fig. 2. We perform a fitting procedure to extract these characteristic quantities from the spectrum. As the first step, the spectrum is divided into two parts, one is for $f \leq f_d$, inspiral and early merger phases, and the other is for $f \geq f_d$, the merger and ringdown phases. f_d is typically chosen as 4 kHz. For $f \leq f_d$, we fit the spectrum by $f^{-1/6}h_0/[1 + \exp\{(f - f_{\text{cut}})/\Delta f\}]$. For $f \geq f_d$, we adopt the Gaussian distribution $h_{\text{peak}} \exp[-(f - f_{\text{peak}})^2/\sigma^2]$. In the fitting, f_{cut} , Δf , h_0 , h_{peak} , f_{peak} , and σ are determined by the χ -square fitting [21].

Figure 3 plots $Gf_{\text{cut}}m_1/c^3$ as a function of compactness of the less massive companion defined by Gm_1/c^2R where R is its circumferential radius. $Gf_{\text{cut}}m_1/c^3$ correlates strongly with Gm_1/c^2R . $Gf_{\text{cut}}m_1/c^3$ depends also on m_0 ; for the larger value of m_0 , it is larger for a given EOS and ν . Note that larger values of m_0 and ν result in smaller values of disk mass (see Fig. 4). Thus, f_{cut} is an indicator that

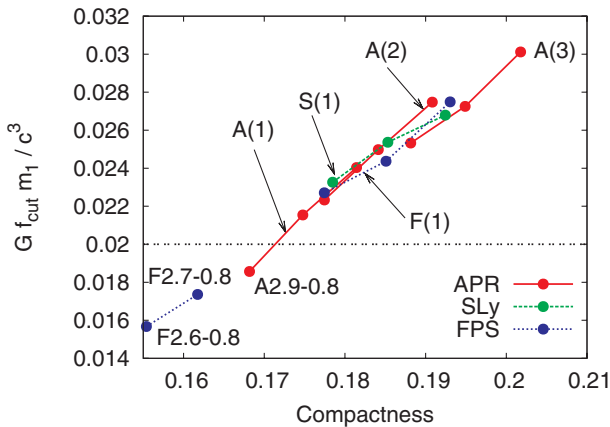


FIG. 3 (color online). $Gf_{\text{cut}}m_1/c^3$ as a function of compactness of a less massive binary component for all the models. Sequence A(1) represents the models A2.9-0.8, A3-0.8, and A3.1-0.8 from left to right. In a similar way, A(2) is a sequence of A2.9-0.9, A3-0.9, and A3.1-0.9, A(3) is A2.9-1, A3-1, and A3.1-1, S(1) is S2.8-1, S2.9-1, and S3-1, and F(1) is F2.6-1, F2.7-1, and F2.8-1. The models below the horizontal line of $Gf_{\text{cut}}m_1/c^3 = 0.02$ can produce disks of mass $\geq 0.01M_{\odot}$.

shows the occurrence of the tidal disruption and possible disk formation. (We note that to obtain $f_{\text{cut}}m_1$, we have to determine m_1 from the gravitational-wave signal in the inspiral phase. However, as discussed in Ref. [22], untangling m_1 and m_2 within the error of 10% may not be an easy task in the case of $m_1/m_2 \sim 1$. It is also worthy to note that R may be determined, if f_{cut} is measured and m_1 is determined; see Ref. [23] for the related topic.)

Figure 4 plots the mass of disk surrounding a BH as a function of σ/f_{peak} . This shows that the disk mass has a positive correlation with σ/f_{peak} . On the other hand, we find that the disk mass does not have a clear correlation with h_{peak} . The disk mass also correlates with $m_0 - M_{\text{thr}}$ and ν : $m_0 - M_{\text{thr}} \lesssim 0.2M_{\odot}$ and $\nu \lesssim 0.8$ appear to be necessary for producing a massive disk with $\geq 0.01M_{\odot}$ (see A2.9-0.8, F2.6-0.8, and F2.7-0.8). The disk mass for other models which do not satisfy this condition is $10^{-3}\text{--}10^{-5}M_{\odot}$ [11,13]. Combination of Figs. 3 and 4 also proposes that a necessary condition for producing a disk of mass $\geq 0.01M_{\odot}$ is $Gf_{\text{cut}}m_1/c^3 \leq 0.02$ and $\sigma/f_{\text{peak}} \geq 0.25$.

The frequency of GWs in the merger phase is slightly outside the most sensitive frequency band of the first and second generation detectors such as LIGO and advanced LIGO (10–1 kHz), because the values of f_{cut} and f_{peak} are $\sim 2.5\text{--}7$ kHz. Nevertheless, the amplitude at $f = f_{\text{cut}}$ and f_{peak} is not extremely small for a hypothetical distance $D = 100$ Mpc. If the proposed third generation detectors such as the Einstein telescope become available with a special design for high-frequency sensitivity, these quantities may be measured. Our results indicate that the formation and evolution processes of a BH and surrounding disk are imprinted in the GW spectrum. Also, GWs are the unique observable which directly carries information of the central region of GRBs. Thus, it is worthy to explore methods for extracting physical information on the merger of BNSs collapsing to a BH from observed GWs, which may clarify the formation process of short GRBs.

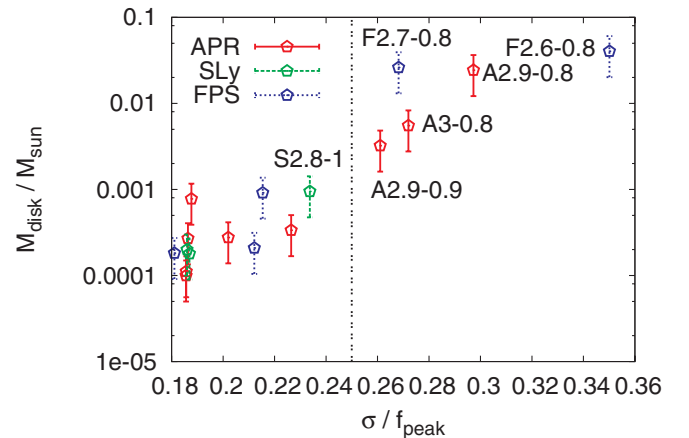


FIG. 4 (color online). Disk mass as a function of σ/f_{peak} for all the models.

Constraining the merger process by GW observation.— As mentioned in the Introduction, the merger hypothesis for the central engine of short GRBs requires that the mass of disk around a BH is greater than $\sim 0.01M_{\odot}$. Our numerical results show that disk mass correlates strongly with σ/f_{peak} and $Gf_{\text{cut}}m_1/c^3$ irrespective of EOS. Assuming that GWs from BNSs are frequently observed, and also, GWs and short GRBs are observed simultaneously for several events in the future, we propose a strategy for exploring the merger hypothesis by analyzing GWs. As a first step, we should determine m_0 , ν , f_{cut} , f_{peak} , and σ for each event: The values of m_0 and ν will be determined from the inspiral waveform using the matched filtering technique [22], and f_{cut} , f_{peak} , and σ from the merger waveform. As a second step, we should infer the disk mass from $Gf_{\text{cut}}m_1/c^3$ and σ/f_{peak} . If the conditions of $Gf_{\text{cut}}m_1/c^3 \leq 0.02$ and $\sigma/f_{\text{peak}} \geq 0.25$ are always satisfied for events in which GWs and short GRBs are simultaneously observed, the merger hypothesis will be strongly supported. Because a small value of $Gf_{\text{cut}}m_1/c^3$ (for the typical mass of neutron stars $1.3\text{--}1.5M_{\odot}$) implies that mass ratio is much smaller than unity, we could conclude that the origin of short GRBs would be the merger of unequal-mass BNSs. By contrast, if simultaneous detections occur irrespective of the values of $Gf_{\text{cut}}m_1/c^3$ and σ/f_{peak} , this does not agree with our numerical results, because these should correlate with the disk mass. In such case, we have to conclude that an unknown mechanism plays a role for producing the GRBs.

Our numerical results indicate that a massive disk is not formed for $\nu \approx 1$ or $m_0 > 3M_{\odot}$ for any EOS. This implies that the merger of BNSs collapsing to a BH does not always produce GRBs. For such case, only GWs will be observed. This suggests another test for the merger scenario.

Finally, a comment is given for the case that an HMNS is formed. Because the HMNS should eventually collapse to a BH via gravitational radiation [11] or angular momentum transport by magnetohydrodynamic effect [14] or neutrino cooling, the HMNS formation scenario can be an alternative in the merger hypothesis. In the HMNS formation, the GW spectrum for the merger phase is significantly different from that in the BH formation because quasiperiodic GWs emitted by a quasiperiodic rotation of the HMNS is likely to produce sharp peaks in the spectrum and characterize the spectrum [11]. In this case, detecting these peaks of GWs will play a crucial role for confirming the merger hypothesis.

Numerical computations were performed on XT4 at the Center for Computational Astrophysics in NAOJ and on NEC-SX8 at YITP in Kyoto University. This work was supported by Grant-in-Aid for Scientific Research (21340051) and for Scientific Research on Innovative Area (20105004) of the Japanese MEXT, by NSF Grant No. PHY-0503366, and by Grant-in-Aid of the Japanese Ministry of Education, Science, Culture, and Sport

(21018008, 21105511).

-
- [1] B. C. Barish and R. Weiss, *Phys. Today* **52**, No. 10, 44 (1999); S. Hild, *Classical Quantum Gravity* **23**, S643 (2006); F. Acernese *et al.* (VIRGO Collaboration), *Classical Quantum Gravity* **19**, 1421 (2002); M. Ando *et al.* (TAMA collaboration), *Phys. Rev. Lett.* **86**, 3950 (2001).
 - [2] R. Narayan, B. Paczynski, and T. Piran, *Astrophys. J.* **395**, L83 (1992).
 - [3] B. Zhang and P. Meszaros, *Int. J. Mod. Phys. A* **19**, 2385 (2004).
 - [4] T. Piran, *Rev. Mod. Phys.* **76**, 1143 (2005).
 - [5] R. D. Blandford and R. L. Znajek, *Mon. Not. R. Astron. Soc.* **179**, 433B (1977).
 - [6] E.g., R. Popham, S. E. Woosley, and C. Fryer, *Astrophys. J.* **518**, 356 (1999).
 - [7] E.g., S. Setiawan, M. Ruffert, and H.-Th. Janka, *Mon. Not. R. Astron. Soc.* **352**, 753 (2004).
 - [8] E.g., J. C. McKinney and C. F. Gammie, *Astrophys. J.* **611**, 977 (2004).
 - [9] E.g., D. B. Fox *et al.*, *Nature (London)* **437**, 845 (2005).
 - [10] S. Kobayashi and P. Meszaros, *Astrophys. J.* **589**, 861 (2003).
 - [11] M. Shibata, K. Taniguchi, and K. Uryu, *Phys. Rev. D* **68**, 084020 (2003); **71**, 084021 (2005); M. Shibata, *Phys. Rev. Lett.* **94**, 201101 (2005); M. Shibata and K. Taniguchi, *Phys. Rev. D* **73**, 064027 (2006).
 - [12] L. Baiotti, B. Giacomazzo, and L. Rezzolla, *Phys. Rev. D* **78**, 084033 (2008).
 - [13] K. Kiuchi, Y. Sekiguchi, M. Shibata, and K. Taniguchi, *Phys. Rev. D* **80**, 064037 (2009).
 - [14] M. D. Duez *et al.*, *Phys. Rev. D* **73**, 104015 (2006); M. D. Duez *et al.*, *Phys. Rev. Lett.* **96**, 031101 (2006); M. Shibata *et al.*, *Phys. Rev. Lett.* **96**, 031102 (2006).
 - [15] R. Oechslin and H. T. Janka, *Phys. Rev. Lett.* **99**, 121102 (2007).
 - [16] A. Akmal, V. R. Pandharipande, and D. G. Ravenhall, *Phys. Rev. C* **58**, 1804 (1998).
 - [17] F. Douchin and P. Haensel, *A&A International* **380**, 151D (2001).
 - [18] B. Friedman and V. R. Pandharipande, *Nucl. Phys. A* **361**, 502 (1981); V. R. Pandharipande and D. G. Ravenhall, in *Proceedings of a NATO Advanced Research Workshop on Nuclear Matter and Heavy Ion Collisions, Les Houches, 1989*, edited by M. Soyeur *et al.*, NATO ASI, Ser. B, Vol. 205, (Plenum Press., New York, 1989), p. 193.
 - [19] E. Gourgoulhon *et al.*, *Phys. Rev. D* **63**, 064029 (2001); K. Taniguchi and E. Gourgoulhon, *Phys. Rev. D* **66**, 104019 (2002); **68**, 124025 (2003); LORENE website: <http://www.lorene.obspm.fr/>.
 - [20] V. Kalogera *et al.*, *Phys. Rep.* **442**, 75 (2007).
 - [21] W. Press, B. P. Flannery, S. Teukolsky, and W. T. Vetterling, *Numerical Recipes in C* (Cambridge University Press, Cambridge, England, 1986).
 - [22] C. Cutler and E. E. Flanagan, *Phys. Rev. D* **49**, 2658 (1994).
 - [23] J. S. Read *et al.*, *Phys. Rev. D* **79**, 124033 (2009).